ELSEVIER

Contents lists available at ScienceDirect

Chemical Engineering Journal

journal homepage: www.elsevier.com/locate/cej

Chemical Engineering Journal

Remediation of wastewaters containing tetrahydrofuran. Study of the electrochemical mineralization on BDD electrodes



A. Urtiaga *, P. Fernandez-Castro, P. Gómez, I. Ortiz

Departamento de Ingenierías Química y Biomolecular, Universidad de Cantabria, Av. de los Castros s/n, 39005 Santander, Spain

HIGHLIGHTS

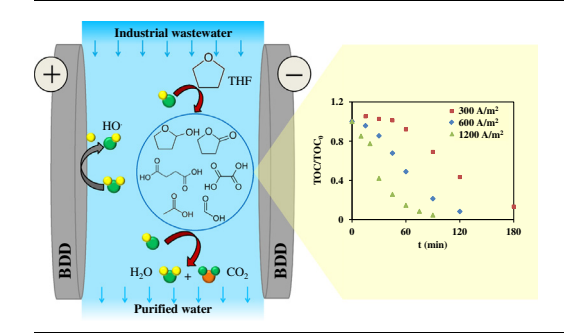
- Remediation of industrial wastewaters by electrochemical oxidation is performed.
- Boron doped diamond electrodes allowed total mineralization of tetrahydrofuran.
- Tetrahydrofuran oxidation pathway is proposed.
- Formation of perchlorate is avoided by operating at low current density.

ARTICLE INFO

Article history:
Received 26 July 2013
Received in revised form 23 October 2013
Accepted 13 November 2013
Available online 23 November 2013

Keywords: Tetrahydrofuran Electrochemical oxidation Boron doped diamond electrodes Industrial wastewaters

G R A P H I C A L A B S T R A C T



ABSTRACT

This work contributes to the development of electro-oxidation on commercial boron doped diamond (BDD) anodes as an efficient and versatile environmental technology to deal with remediation of tetrahydrofuran (THF) polluted industrial wastewaters. Working with an undivided flow-by electrochemical cell, a systematic experimental study has been carried out to analyze the influence of the following operation variables: (i) initial THF concentrations in the range 500-1100 mg/L, (ii) supporting electrolyte, Na₂SO₄ and NaCl and (iii) current density in the range 300-1200 A/m². The performance of the oxidation process was assessed through the change in the concentration of THF, Chemical Oxygen Demand (COD), and Total Organic Carbon (TOC) being the current density the variable that exerted the most positive kinetic influence; more precisely the reduction of COD after 60 min changed from 40% at j_{app} = 300 A/m² to 95.5% at $j_{app} = 1200 \text{ A/m}^2$, whereas the reductions of TOC were typically higher than 95% for a value of the specific charge of Q = 10 A/h L. Besides, THF oxidation products have been analyzed, and the reactions' pathway are proposed. Finally, the formation of chloride by-products, such as perchlorate was assessed observing that it was hindered at low current densities. In the view of these findings, it is concluded that THF oxidation on BDD anodes should be better performed at low current densities, i.e. 300 A/m² for the type of wastewaters analyzed in the present work, to reach a compromise between effective degradation and the formation of undesirable chlorinated by-products.

© 2013 Elsevier B.V. All rights reserved.

1. Introduction

Tetrahydrofuran (THF) is used in a wide range of applications in the chemical industry: as solvent and raw material in the manufac-

Abbreviations: Tetrahydrofuran, THF; Boron doped diamond, BDD; Chemical Oxygen Demand, COD; Total Organic Carbon, TOC; γ -butyrolactone, GBL; 2-hydroxy tetrahydrofuran, 2-OHTHF.

* Corresponding author. Tel.: +34 942 201587. E-mail address: urtiaga@unican.es (A. Urtiaga). turing and processing of polymers [1], as reagent for drug and chemical synthesis [2], and so on. The synthesis of adipic acid and the production of synthetic rubbers are examples of large scale applications of THF. The demand of THF is growing annually and the global market is projected to exceed 800 thousand tons by 2017 [3]. The THF properties of miscibility with water and high vapor pressure facilitate its transference to surface waters, ground waters and atmosphere [4]. THF presence in the environment is associated with risks to both human and animal health. Its effects

to the central nervous system and liver, as well as its carcinogenicity have been recently assessed. The US Environmental Protection Agency has estimated a human oral reference dose (RfD) of 0.9 mg THF/kg-day; higher exposures are likely to be associated with adverse health risks [5]. For these reasons the presence of THF in industrial effluents should be strictly controlled and the removal of THF from wastewaters is required.

With the aim of treating wastewaters containing THF, different processes and techniques have been evaluated. THF degradation studies carried out using activated sludge concluded that THF was not easily biodegradable [6]. It was also found that THF negatively affected the activity of all-purpose secondary treatments, reducing the effectiveness of the general organic material degradation [7]. Recent research in the field of biodegradation has been focused to the search of novel bacteria able to completely mineralize THF concentrations in waters with an initial THF content of 30 mM [8,9]. However, the reported studies showed several limitations from a practical point of view, among them in the performed studies THF was the sole carbon and energy source [10], and it was difficult to recover the biomass from the treated waters [11].

The separation of THF-water mixtures is usually aimed at the recovery of the solvent. Atmospheric distillation is limited by the formation of an azeotrope at 6.5% water mass fraction [12]. Further THF dehydration requires the use of extractive distillation [13] or other advanced separation processes, e.g.: pervaporation [14] and liquid-liquid extraction using ionic liquids [15]. The difficulty of using membranes for the selective permeation of THF from aqueous solutions lies in the polar nature of this organic compound, and therefore, its low affinity towards the organophilic rubbery membranes usually employed for the removal of volatile compounds from residual waters [16]. Pervaporation membranes obtained from glassy polymers were characterized [17], although the poor values of THF flux through the membrane would hinder its practical implementation.

Chemical technologies are usually preferred by the process industry to treat wastewaters, due to their high removal efficiency and robustness to be adapted to changing operating conditions. However, only a few works deal with the removal of THF in wastewaters by means of chemical treatments. Although the chemical oxidation of THF has been extensively studied [18-21], most of the works were focused on obtaining the oxidation products, namely, 2-hydroxytetrahydrofuran and γ-butyrolactone (GBL). GBL is used in a wide range of applications such as intermediate in the synthesis of N-methylpyrrolidone, herbicides, pharmaceuticals and even in the electronics field [22]. Among that group of references, the selective anodic oxidation of THF on Pt anodes in acidic media was reported. THF in highly loaded wastewaters was degraded by catalytic aqueous phase reforming, with the aim of producing hydrogen as a product of the treatment process [23]. Mehrvar et al. [24,25] studied the kinetics of the photocatalytic degradation of THF in low concentrated aqueous solutions, together with the identification of the oxidation products.

Electrochemical oxidation using boron doped diamond (BDD) electrodes can overcome the limiting oxidizing abilities of conventional advanced oxidation processes [26]. The properties of BDD promote the generation of hydroxyl radicals [27], a non-selective and very powerful oxidant, with a high standard reduction potential (2.80 V vs. SHE). Due to the weak interaction between electrogenerated hydroxyl radicals and the BDD anode surface, the side reaction towards oxygen evolution is slower than their reactivity towards organic compounds [28,29]. Furthermore, BDD anodes have a high overpotential for the oxygen evolution reaction (1.3 V) compared with the platinum anode (0.3 V). The ability of BDD to mineralize a wide range of recalcitrant organic compounds and actual wastewaters were reviewed by Panizza and Cerisola [27] and Anglada et al. [26]. Relevant to the present work the deg-

radation of carboxylic acids [30,31], landfill leachates [32,33], industrial saline wastewaters [34,35], emerging contaminants [36,37] and reverse osmosis concentrates [38] are highlighted.

This research investigates the effectiveness of electrooxidation using boron-doped diamond electrodes for oxidizing and mineralizing THF contained in industrial wastewaters characterized by a high load of the organic contaminant, e.g.: THF in the range 500–1100 mg/L. The effects of current density, type of electrolyte, and initial THF concentrations on reaction rates were studied. The identification of the intermediates was conducted and the electrochemical degradation pathway was proposed. The formation of chlorinated oxidation by-products was also assessed. In the above view, the operating conditions for the efficient and safe electrochemical decomposition of THF in industrial wastewaters are proposed.

2. Materials and methods

Process wastewaters from a rubber manufacturing company were used in the experimental work, with the following general characteristics: pH = 7.1, conductivity = $20 \,\mu\text{S/cm}$, total dissolved solids: 9.1 mg/L. Typically, THF concentrations in this type of industrial waters are in the range $450\text{--}1200 \,\text{mg/L}$. In the present work, the initial tetrahydrofuran concentration was leveled to 500 and $1100 \,\text{mg/L}$ by adding extra THF (HPLC grade, Panreac). The low conductivity of the wastewaters required the addition of a supporting electrolyte. Sodium chloride (PA-ACS-ISO Panreac) and sodium sulfate (Panreac) were tested as electrolytes in order to compare their effect on THF mineralization. The initial NaCl concentration was fixed at 1 g/L to provide a conductivity of approximately $2000 \,\mu\text{S/cm}$. The amount of Na_2SO_4 was selected in order to reach the same initial conductivity as when using NaCl, resulting in $1.3 \,\text{g/L}$ of Na_2SO_4 .

Electrochemical experiments were performed at laboratory scale in a DiaCell 201 PP (Adamant Technologies, Switzerland) system comprised of two rectangular flow channels, separated by a bipolar electrode (Fig. 1). All anode, cathode and bipolar electrode consist of a boron-doped diamond (BDD) coating on a silicon plate, with circular shape. The total anodic area was $140 \, \text{cm}^2$ (70 cm² each anode × 2 anodes) with an interelectrode gap between anode and cathode of 1 mm. Two power supplies were used: a Vitecom 75-HY3005D (with a maximum output of 5 A and 30 V) and a GW Instek GPR-6015D (with a maximum output of 15 A and 60 V). The system was also formed by a feed vessel, a recirculation pump (Iwaki Magnet MD-20R-220N) and a cooling system. The feed temperature was maintained at 293 K. A volume of 1 L of feed water was loaded in the jacketed feed tank and recirculated at a flow rate of 600 L/h (300 L/h through each cell compartment).

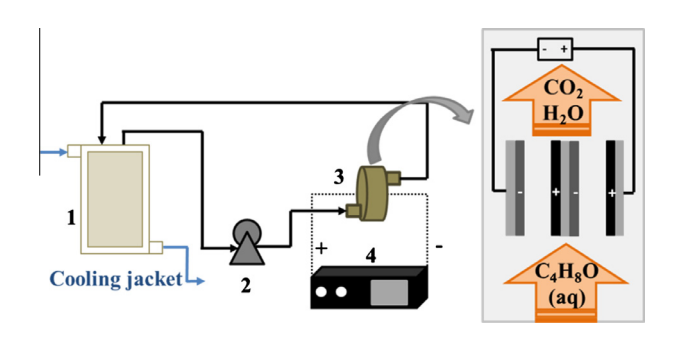


Fig. 1. Electrochemical set-up formed by the thermostatized feed tank (1), pump (2), BDD electrochemical cell (3) and power supply (4).

Aqueous samples were withdrawn from the feed tank at different times during the electrochemical process. The concentrations of THF and organochlorinated compounds were analyzed using gas chromatography with mass spectrometry detector. An Agilent GC 6890 series equipped with a headspace autosampler and a DB-624 column was used. The concentrations of γ -butyrolactone (GBL) and 2-hydroxytetrahydrofuran were analyzed using a gas chromatography (GC-2010 Plus, Shimadzu) equipped with mass spectroscopy detector, autosampler, autoinjector and column HP-5ms. Finally, the solvent used for aqueous samples extraction prior to gas chromatography was dichloromethane (Lichrosolv®). The concentrations of chloride, chlorate, perchlorate and of the carboxylic acids obtained as THF decomposition products were measured using an ICS-110 (Dionex) ion chromatograph with a conductivity detector provided with an AS9-HC column. Solutions of Na₂CO₃ (9 mM) in water were used as the mobile phase, based on Standard Methods 4110 B [30]. Total Organic Carbon (TOC) was analyzed in a TOC-VCPH Shimadzu equipped with an automatic sample injector ASI-V.

Chemical Oxygen Demand (COD) was measured following a closed reflux colorimetric method, according to Standard Methods 5220D [39]. Free chlorine was measured using N,N-diethyl-p-phenylenediamine (DPD) reactive with a DR/890 colorimeter.

Different standards were purchased to identify the intermediates obtained during THF oxidation, and to prepare calibration curves: γ -butyrolactone (\geqslant 99%, Sigma–Aldrich), 2-hydroxytetrahydrofuran (Sigma–Aldrich), succinic acid (\geqslant 99%, Fluka), malonic acid (\geqslant 99%, Merck), fumaric acid (99% PS, Panreac), glacial acetic acid (99.5%, Panreac), formic acid (98%, Panreac), oxalic acid (COOH)₂·2H₂O (100%, Panreac).

3. Theory

Several mathematical models that describe the processes occurring in the anodic oxidation of organic compounds by means of boron doped diamond electrodes have been developed. Panizza et al. [40] developed a simple mathematical model that only considered direct and/or hydroxyl radical mediated oxidation of organic contaminants. The model defines two different operating regimes depending on the applied current density (j_{app}) to the limiting current density (j_{lim}) for COD ratio. The latter can be calculated by means of the following expression:

$$\mathbf{j}_{lim} = 4k_m \cdot F \cdot COD(t) \tag{1}$$

where j_{lim} is the limiting current density for organics mineralization (A/m^2) , F is Faraday's constant (96,485 C/mol), k_m is the mass transport coefficient (m/s), COD is the Chemical Oxygen Demand (mol/m^3) and 4 is the number of exchanged electrons.

The following operating regimes are identified in this model:

j_{app} < j_{lim}, the electrolysis is under current control. In this operating regime COD decreases linearly with time, according to Eq. (2),

$$COD(t) = COD_0 \left[1 - \frac{\alpha \cdot A \cdot k_m}{V} \cdot t \right]$$
 (2)

where $\alpha = j_{app}/j_{lim}$, $A~(\text{m}^2)$ is the anodic area and $V~(\text{m}^3)$ is the volume treated.

 j_{app} > j_{lim}, the electrolysis is under mass transport control and COD removal follows an exponential trend,

$$COD(t) = COD_0 \cdot \exp\left[-\frac{A \cdot k_m}{V} \cdot t\right]$$
 (3)

When there is a change in the kinetic regime during the electrochemical treatment, a combination of zeroth order and first order kinetics will be observed, described by Eqs. (2) and (4),

$$COD(t) = \alpha COD_0 \cdot \exp\left[-\frac{A \cdot k_m}{V} \cdot t + \frac{1 - \alpha}{\alpha}\right] \tag{4}$$

The time at which the applied current equals the limiting current is called critical time (t_{cr}) that is calculated according to

$$t_{cr} = \frac{1 - \alpha}{\alpha} \cdot \frac{V}{A \cdot k_m} \tag{5}$$

The previous model formed by Eqs. (2)–(5)is usually able to predict the behavior of the system as long as indirect oxidation processes do not take place. Cañizares et al. [31] and Mascia et al. [41] proposed models that describe the oxidation of organics not only by means of hydroxyl radicals near the anode surface, but also in the bulk by means of electrogenerated oxidants, i.e.: active chlorine and hydrogen peroxide. Urtiaga et al. [42] went a step further by modeling the combined oxidation on BDD anodes of organic compounds and ammonia contained in landfill leachates by means of both direct and chlorine mediated indirect oxidation.

The contribution of indirect oxidation processes on the overall COD removal rate can be described by the following simplified model,

$$COD(t) = COD_0 \cdot \exp[-(k_1) \cdot t] = COD_0 \cdot \exp\left[-\left(\frac{A \cdot k_m}{V} + k\right) \cdot t\right]$$
 (6)

where k is a pseudo first order kinetic constant that will depend on the same variables as the concentration of inorganic oxidants does, such as current density. It can be assumed that indirect oxidation processes gain relevance only under mass transport control.

The value of the mass transfer coefficient k_m for the system under study can be calculated using the correlation reported in a previous work [33], that applied the limiting-current technique based in the oxidation of $[Fe(CN)_6]^{3-}/[Fe(CN)_6]^{4-}$ redox couple using an electrochemical cell with the same dimensions as the cell used in the present work,

$$Sh = 0.54Re^{0.385} \cdot Sc^{0.20} \tag{7}$$

where Sh is Sherwood number $(k_m \cdot d_e \cdot D^{-1})$, Sc is Schmidt number $(\mu \cdot \rho^{-1} \cdot D^{-1})$ and Re is Reynolds number. For the circular electrochemical cell with variable cross section along the fluid pathway, the minimum value of the Reynolds number is given by $Re = 2Q \cdot \rho \cdot d^{-1} \cdot \mu^{-1}$ [33].

The diffusivity of THF in water was calculated using the Wilke–Chang correlation [43], D_{THF} (293 K) = 1.05×10^{-9} m²/s. Considering that all experiments were performed working with a flow rate through the cell of Q = 300 L h^{-1} and constant temperature of 293 K, the resulting value of the mass transfer coefficient is $k_m = 2.0 \times 10^{-5}$ m s⁻¹. Therefore, working with initial COD values of 3 and 1.5 g/L, the calculated limiting current densities are 720 and 360 A/m² respectively.

4. Results

4.1. Influence of the electrolyte

Sodium chloride (NaCl) and sodium sulfate (Na₂SO₄) were tested as electrolytes in order to compare their effect on THF mineralization. From the point of view of the industrial case study, NaCl was preferred due to its easier availability at the production site. Fig. 2 shows the evolution of COD and TOC for the electrooxidation of a feed water with the following initial characteristics: [THF]₀ \approx 1100 mg/L; [COD]₀ \approx 3000 mg/L; [TOC]₀ \approx 800 mg/L, at two values of the applied current density, 300 and 1200 A/m².

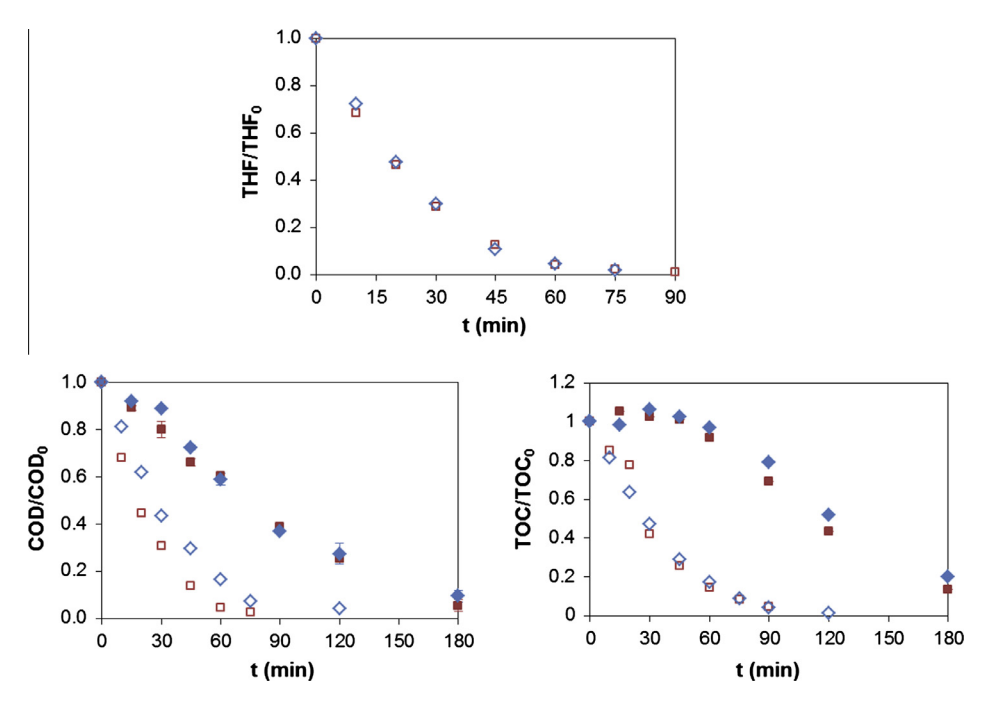


Fig. 2. Evolution with time of normalized THF, COD and TOC using NaCl 1 g/L, $j_{app} = 300 \text{ A/m}^2$ (■) and $j_{app} = 1200 \text{ A/m}^2$ (□); and Na₂SO₄ 1.3 g/L, $j_{app} = 300 \text{ A/m}^2$ (♦) and $j_{app} = 1200 \text{ A/m}^2$ (♦). [THF]₀ = 1100 mg/L, COD₀ ≈ 3000 mg/L.

Most experiments were performed on a duplicate basis, with very good reproducibility as it depicted in the small error bars shown in Fig. 2. It should be noted that the limiting current density, calculated using Eq. (1) for the initial $COD_0 \approx 3000 \ mg/L$ employed in the experiments was $j_{lim} = 720 \text{ A/m}^2$. At low current density, j_{app} = 300 A/m², COD and TOC removal rates were equivalent for both electrolytes, and the development of COD showed a linear trend, typical of electrochemical processes under current control. Working above the limiting current density, $j_{app} = 1200 \text{ A/m}^2$, shows that also THF removal rates were equivalent for both electrolytes, although removal kinetics turned faster to first order kinetics. This fact suggests that the free chlorine derived from chloride oxidation did not contributed to the oxidation of THF and its oxidation by-products, and that hydroxyl radicals are most likely to be the major contributors to the mineralization of the organic load present in the wastewaters.

Fig. 3 shows the behavior of pH as a function of the electrolyte. pH was monitored, since its value needs to be controlled in the

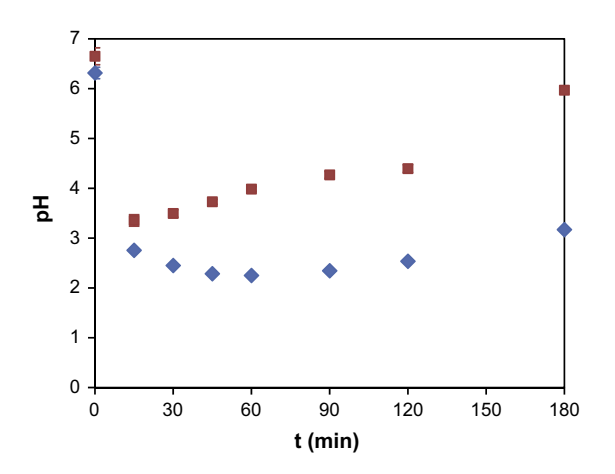


Fig. 3. Evolution of pH with time for NaCl (\blacksquare) and Na₂SO₄ (\blacklozenge) as electrolytes. $j_{app} = 600 \text{ A/m}^2$ and COD₀ $\approx 3000 \text{ mg/L}$.

treated industrial waters [44]. When using NaCl the value of pH initially decreased and later on recovered its initial value after 180 min of treatment, while when using Na₂SO₄ as electrolyte, the pH decreased to a value of 3 and remained at acidic pH ranges. Therefore, in terms of pH, the use of NaCl is also more favorable than Na₂SO₄ because in the latter case the treated water would need to be amended before its release. It will be seen later that along with the electrochemical oxidation of THF, several organic acids were produced, that is the most likely reason of pH decreasing sharply as soon as the oxidation process starts and recovering the initial value when organic acids were degraded. Considering these experimental findings, and its easier availability, NaCl was selected as supporting electrolyte.

4.2. Influence of the applied current density

The influence of the applied current density was studied in the range of j values of 300, 600 and 1200 A/m². Experimental data of the change of THF, COD and TOC are depicted in Fig. 4. Experiments were conducted with initial THF and COD concentrations of 1100 mg/L and 3000 mgO₂/L respectively, and the calculated value of the limiting current density, according to Eq. (1) is $j_{lim} = 720 \text{ A/m}^2$. It is observed that at low $j_{app} = 300 \text{ A/m}^2$ THF oxidation initially showed zeroth order kinetics to become later exponential, and for high $j_{app} = 1200 \text{ A/m}^2$, the kinetics of THF oxidation displayed an exponential trend with time. Nevertheless, a small influence of the applied current on the kinetics of THF oxidation was observed. On the contrary, the effect of the applied current on COD and TOC evolutions is notorious. The reduction of both parameters was highly enhanced at higher applied current densities, although important differences can be observed in the kinetic trends. In the case of COD, at $j_{app} = 300 \text{ A/m}^2$, a value clearly under the limiting current density, the change is initially linear to become exponential only after more than 60% of COD was removed. Increasing the applied current density to 600 A/m² made COD elimination faster and the kinetic trend became exponential. The increase of j_{app} to 1200 A/m² improved further the removal of COD, pointing to the contribution of indirect oxidation processes

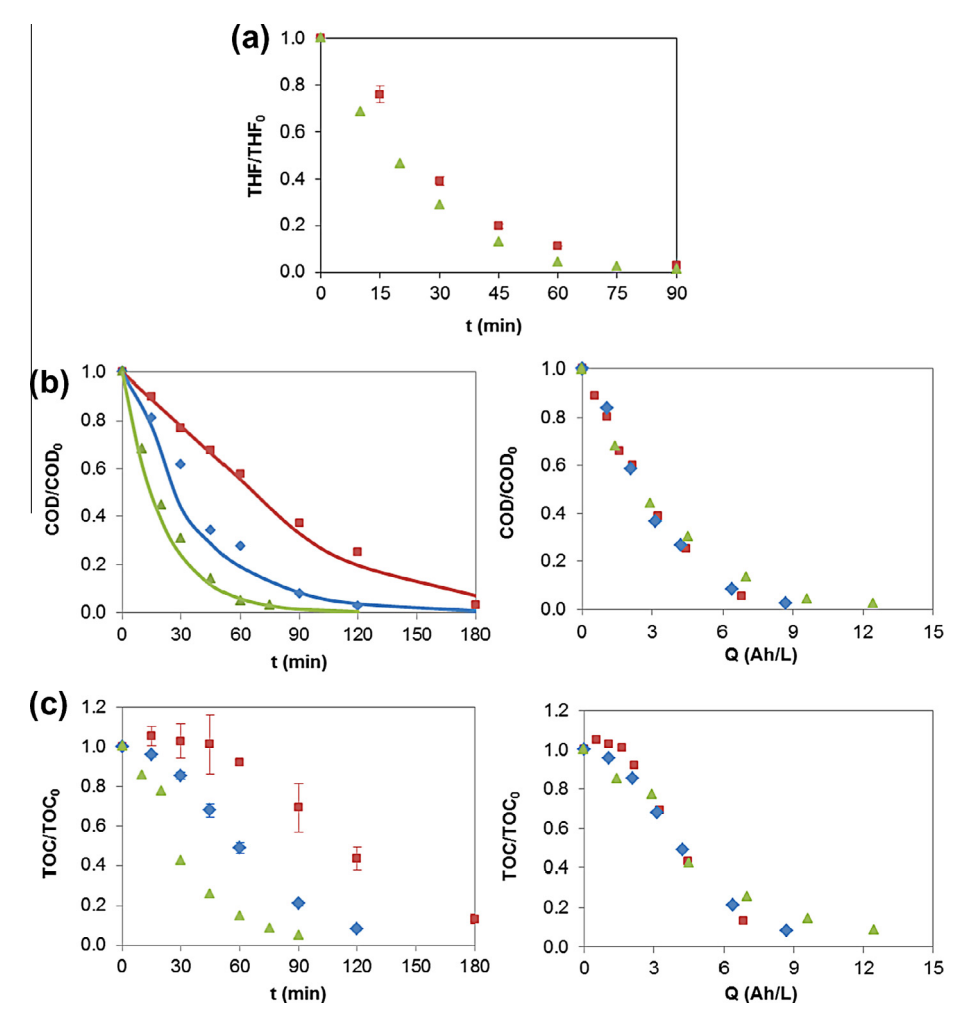


Fig. 4. Evolution of normalized THF (a), COD (b) and TOC (c) for $j_{app} = 300 \text{ A/m}^2$ (\blacksquare), $j_{app} = 600 \text{ A/m}^2$ (\clubsuit). Data are presented as a function of time and as a function of the specific charge passed, Q. [THF]₀ $\approx 1100 \text{ mg/L}$, [COD]₀ $\approx 3000 \text{ mg/L}$, 1 g/L NaCl electrolyte solution. Solid lines represent the simulated normalized COD. THF data only available at 300 and 1200 A/m².

with participation of hydroxyl radicals and other electrogenerated active oxidant species.

Concerning the experimental data of TOC evolution (Fig. 4c), working at a low applied current density of 300 A/m² an initial plateau was observed, so during a period of one hour the TOC value remained at the initial value. As it will be seen later, THF oxidation reactions produce compounds with an increase of the oxidation grade (higher number of oxygen atoms) while the number of carbon atoms remains constant. This fact likely explains the reason of keeping constant the initial TOC concentration. By increasing the applied current density the plateau was shortened. On the other hand, higher applied current densities resulted in faster TOC removal rates.

COD and TOC values are also presented as a function of the specific electrical charge *Q*,

$$Q = j \cdot A \cdot t/V \tag{8}$$

that depends on the anode area (A), the current density (j), the volume of effluent treated (V) and the treatment time (t). It is observed that COD and TOC evolutions obtained at different current densities are overlapped. This means that the current efficiency is similar at any of the applied conditions. Also, the instantaneous current efficiency, ICE, calculated as given by Eq. (9) is plotted in Fig. 5,

$$ICE_{COD} = \frac{4F \cdot V}{I} \cdot \frac{[COD_t - COD_{t+\Delta t}]}{\Delta t} \tag{9}$$

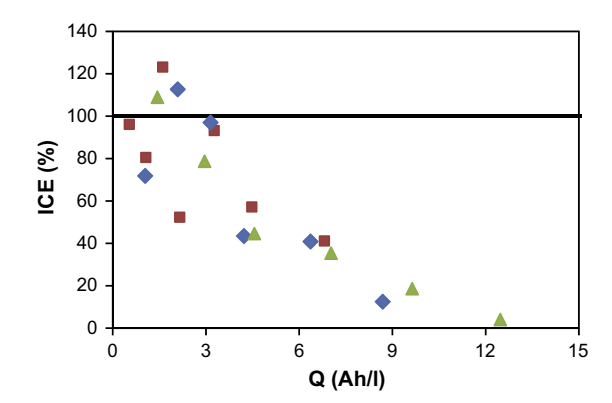


Fig. 5. Effect of current density on the instantaneous current efficiency, $j_{app} = 300 \text{ A/m}^2$ (\blacksquare), $j_{app} = 600 \text{ A/m}^2$ (\spadesuit) and $j_{app} = 1200 \text{ A/m}^2$ (\blacktriangle). [COD]₀ $\approx 3000 \text{ mg/L}$, 1 g/L NaCl electrolyte solution.

where I is the applied current (A), and COD_t , $COD_{\Delta t}$ are the concentration of COD at time t and Δt , respectively At low values of the specific charge, ICE maintains an average value of 100%, which is the ideal situation. It can be observed that the applied charge does not significantly influence on the instantaneous current efficiency.

Alongside with the variation of the applied current density, a change of the cell voltage was observed. Energy consumption (W,

kW h/m³) is directly proportional to the specific electrical charge passed Q defined by Eq. (8) and to the cell potential (ν , V), as shown in the following equation:

$$W = Q \cdot v \tag{10}$$

For the data shown in Fig. 4, experiments performed at $j_{app} = 300 \, \text{A/m}^2$ resulted in a cell voltage of 16.5 V, and for $j_{app} = 1200 \, \text{A/m}^2$, the cell voltage was 28.6 V. The energy consumption increased with current density, e.g.: an increase in current density from 300 to 1200 A/m^2 resulted in an increase of the specific energy consumption needed to reduce the concentration of COD to the discharge limit (COD < 200 mg/L) from 39.3 to 105.9 kW h/kgCOD.

The use of NaCl as electrolyte may produce other inorganic and organic species in the reactive medium due to the high electrochemical reactivity of chloride [45,46], so the effect of the applied current density on the evolution of the inorganic chlorine species

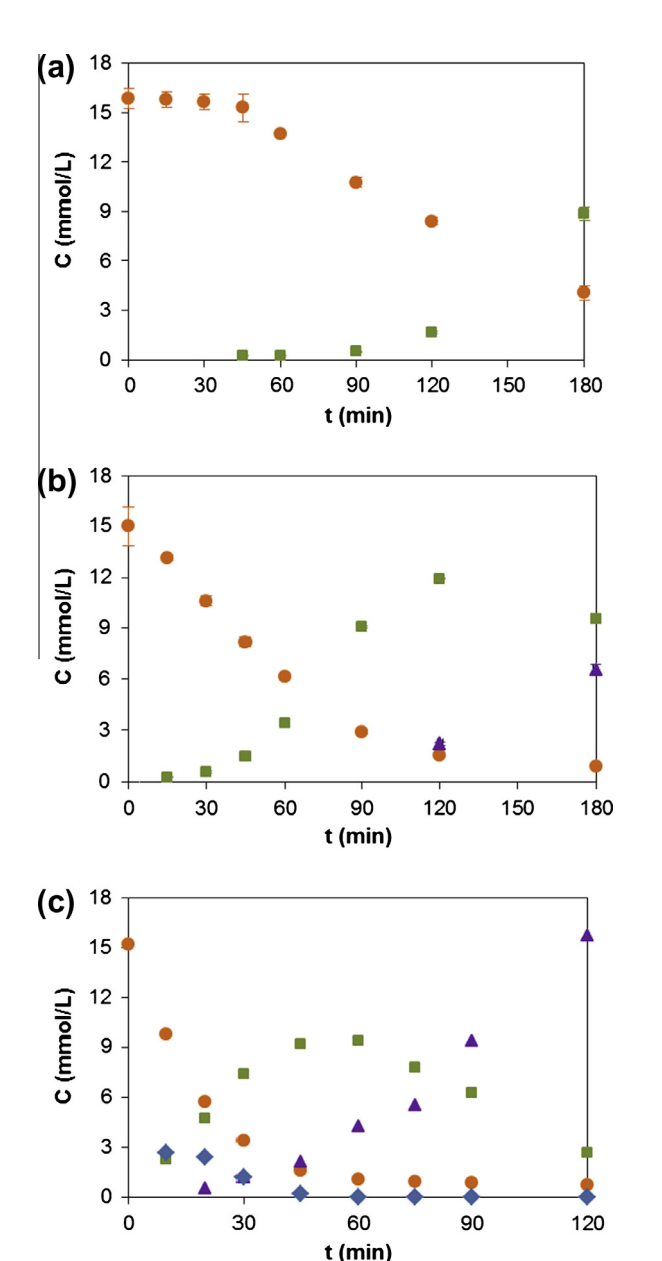


Fig. 6. Evolution with time of Cl^- (\blacksquare), free chlorine (\blacklozenge), ClO_3^- (\blacksquare) and ClO_4^- (\blacktriangle) working at j_{app} 300 A/m² (a), 600 A/m² (b) and 1200 A/m² (c) using 1 g/L NaCl electrolyte and $COD_0 \approx 3000 \text{ mg/L}$.

was studied. Fig. 6 shows the evolution of chloride, free chlorine (data only available at $j_{app} = 1200 \text{ A/m}^2$), chlorate and perchlorate. It is observed that in all cases, chloride concentration diminished with time, while it was transformed into chlorate, a species that conducts as an intermediate product, and finally to perchlorate. Interestingly, Fig. 6a indicates that when a low current density was applied (300 A/m²), chlorate was produced only after a long period of treatment, when TOC was less than half of its initial value [47]. At higher applied current densities, chlorate formation began sooner as a consequence of the much faster removal of organic compounds. This behavior can be explained considering that the use of BDD anodes promotes the generation of hydroxyl radicals and COD is oxidized primarily. Chlorine evolution is enhanced at lower COD concentrations then causing the formation of chlorate. Furthermore, due to the higher current availability, the oxidation reaction from chlorate to perchlorate may happen. In our experimental study, perchlorate formation was observed at j_{app} = 600 A/m² and it was particularly enhanced at j_{app} = 1200 A/m², while it was not detected when working at low current density of 300 A/m². The delayed formation of perchlorate in presence of organic matter and at low intensity has been reported in a previous work about the electrooxidation of landfill leachates [45,48].

The formation of chlorate and, above all, perchlorate are not recommended due to the fact that they confer health risks, such as carcinogenic potential [49]. Once COD and TOC values were low, and THF was removed, the main species present in the solution (as it will be seen later) are organic acids of short chain. Therefore, the electrochemical treatment could be integrated with a subsequent biological process in a way that allows economic removal of the organic acids hindering the formation of chlorate and perchlorate.

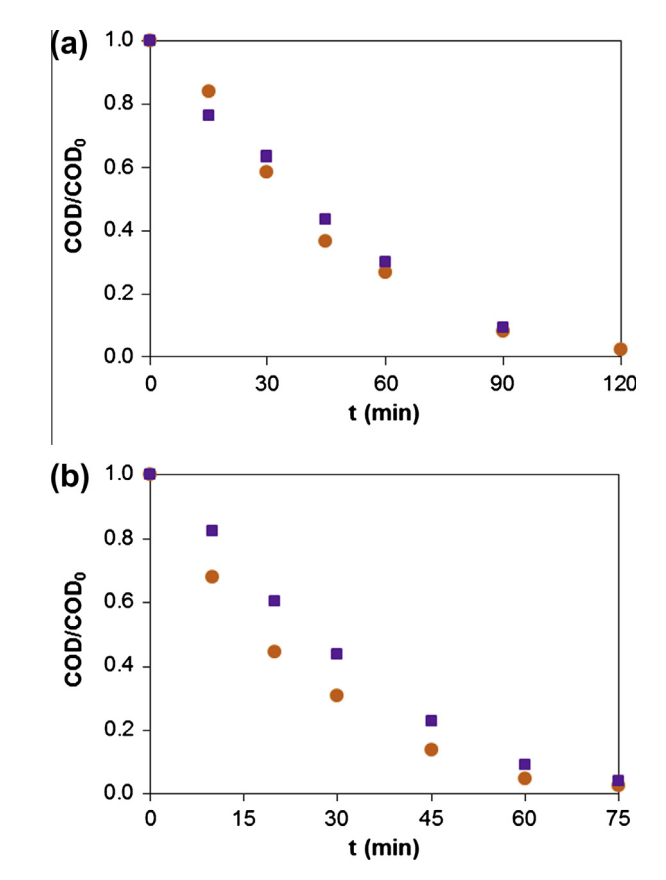


Fig. 7. Influence of COD₀ working at $j_{app}|j_{lim}=0.8$ (a) and $j_{app}|j_{lim}=1.8$ (b). [THF]₀ = 1000 mg/L, COD₀ \approx 3000 mg/L () and [THF]₀ = 550 mg/L, COD₀ \sim 1500 mg/L ().1 g/L NaCl electrolyte solution.

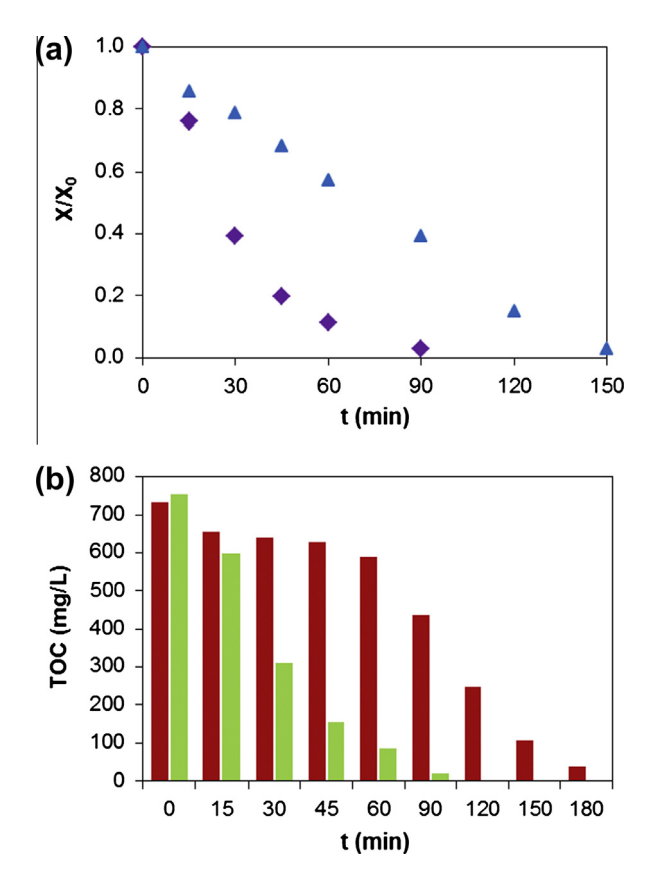


Fig. 8. Evolution with time of normalized concentration of THF (\blacklozenge) and COD (\blacktriangle) (a); TOC measured (\blacksquare) and TOC calculated from THF data (\blacksquare) (b). COD₀ \approx 3000 mg/L, $j_{app} = 300 \text{ A/m}^2$, 1 g/L NaCl electrolyte solution.

4.3. Influence of initial COD

Typically, the organic contaminant load of the industrial wastewater will vary as a function of the process operating conditions. In

order to study the influence of the initial COD concentration, water samples were spiked with THF to provide two initial COD values: 3000 mg/L and 1500 mg/L. When dealing with $COD_0 = 1500$ mg/L, experiments were performed at j_{app} 300 and 600 A/m², while for $COD_0 = 3000 \text{ mg/L } j_{app}$ was 600 and 1200 A/m². COD change with time was plotted as a function of the applied current to the limiting current ratio (Fig. 7). At j_{app}/j_{lim} < 1, the trends of the normalized COD evolution are overlapped, and the influence of the initial COD concentration was negligible. Nevertheless, at $j_{app}/j_{lim} = 1.8$ (Fig. 7b), COD reduction was slightly faster when the initial COD concentration was 3000 mg/L. It is important to highlight that in the latter conditions the difference j_{app} – j_{lim} was about 500 A/m², while in the experiments performed using an initial COD concentration of 1500 mg/L, the difference j_{app} – j_{lim} was approximately 280 A/m². The higher excess of applied current over the limiting one promoted the generation of higher oxidant concentration and, consequently, it was translated in a faster removal rate due to indirect oxidation mechanisms as given by Eq. (6) of theory section.

4.4. Study of transformation products

With the aim of studying the oxidation pathway of THF during the electrochemical oxidation, a detailed analysis of the intermediate compounds evolution was performed. With this purpose, soft electro-oxidation conditions were selected. By applying a low current density it was previously shown that the mineralization rate was slowed down, so it was expected that the presence of intermediate compounds would be easier to be analyzed. A new experiment using ultrapure water spiked with 1000 mg/L THF, NaCl as electrolyte and a current density of 300 A/m² was performed. The reason of using ultrapure water as background solvent was to avoid interferences due to the unknown detailed organic content of the process water.

Fig. 8a depicts the development of the normalized COD and THF concentration. As it is shown, THF reached less than 30 mg/L after 90 min. Nevertheless, COD values were still relatively high and it was necessary 150 min to reach values of COD close to zero. Fig. 8b compares the experimental values of TOC with the

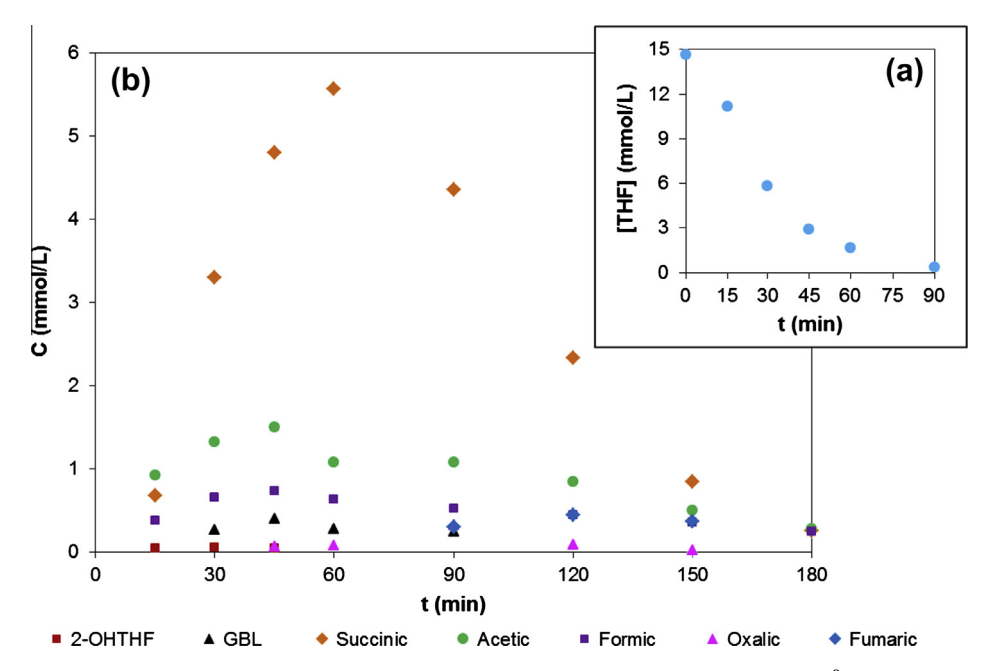


Fig. 9. Evolution of (a) THF and (b) intermediate compounds involved in the THF electrochemical oxidation. $j_{app} = 300 \text{ A/m}^2$, COD₀ $\approx 3000 \text{ mg/L}$, 1 g/L NaCl electrolyte solution.

Fig. 10. Proposed pathway for the electrochemical degradation of tetrahydrofuran on BDD anodes.

theoretical TOC calculated for the analyzed THF concentration. The large differences observed indicate that THF was not directly converted into $\rm CO_2$; instead, smaller organic molecules were formed as intermediates.

The main organic intermediates identified in our research during the electrochemical oxidation of THF using BDD electrodes were 2-hydroxy tetrahydrofuran (2-OHTHF), γ -butyrolactone (GBL), succinic acid, fumaric acid, oxalic acid, acetic acid and formic acid. The development of these compounds is depicted in Fig. 9. The oxidized forms of the cyclic furan, 2-OHTHF and GBL, were detected in low concentrations and mainly at the initial stages of the oxidation process. The main oxidation product was succinic acid, that results from the opening of the cyclic GBL. Other smaller carboxylic acids such as acetic, oxalic and formic acids, together with small amounts of fumaric acid were also detected. The analysis of maleic and malic acids was included in the analytical method, but those acids were not detected in the samples.

Previous studies on the electro-oxidation of THF on Pt anodes [20,21] focused to the production of GBL, reported that succinic and formic acids were also formed as by-products. Mehrvar et al. [24] also found that during the ${\rm TiO_2}$ photocatalytic degradation of aqueous THF the main intermediates were 2-hydroxytetrahydrofuran, γ -butyrolactone, succinic acid and formic acid. On the other hand, Bensalah et al. [30] studied the electrochemical oxidation of succinic acid on BDD and they found that glycolic, glyoxylic, fumaric and maleic acids were formed. Nevertheless, they proposed that these acids were oxidized through a rapid and non-selective way into oxalic and formic acids.

Identification of intermediates formed in the galvanostatic electrolysis of THF allowed the definition of a simple mechanistic model for THF oxidation (Fig. 10). First, THF is oxidized to 2-hydroxy tetrahydrofuran by adding a hydroxyl group into the cycle furan. After that, a double link occurs between the hydroxyl group and the carbon atom to form γ -butyrolactone. The concentration of both compounds is small, as shown in Fig. 9, because they are formed and consumed rapidly. The next step is the opening of the cycle, to give succinic acid. Succinic acid is the intermediate found at highest concentrations. Succinic acid could form fumaric acid or be degraded into short chain compounds such as oxalic, acetic or formic acids. Fumaric acid was only found after 90 min of electrochemical treatment after a maximum of the concentration of succinic acid, precursor of fumaric acid.

Fig. 11 plots ΔTOC defined as the difference between the value of TOC experimentally measured, TOC_m , and the value of TOC_t calculated from the concentrations of THF and the identified intermediate products. It is observed that regardless the strong analytical effort, the TOC balance does not fully match. Initially, when the THF concentration is high and the main intermediates follow the oxidation pathway previously described, theoretical TOC (mass balance of the quantified intermediates) equals measured TOC. However, at intermediate times there is a maximum difference around 170 mg/L between measured and theoretical TOC which indicates that there are other organic intermediates compounds that we were not able to identify by the experimental procedure and analytical techniques used. Nevertheless, the maximum value of ΔTOC is less than 23% of the initial TOC, and at the end of the experiment the difference between measured and theoretical TOC is less than 4% the initial value.

One possible reason for the observed ΔTOC could be the formation of volatile compounds [50]. The major organochloride intermediates identified were 1,1-dichloroethylene, dichloromethane, chloroform, tetrachloromethane, dichloroacetic acid, 1,2-dichloroethane, trichloroethylene and 1,1,2-trichloroethane. The profile of the intermediates generated at 300 A/m² is shown in Fig. 12,

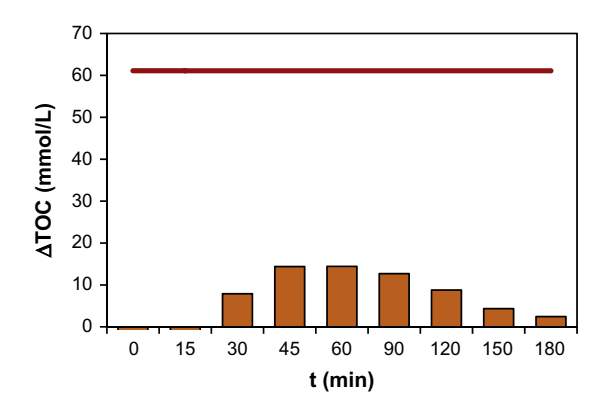
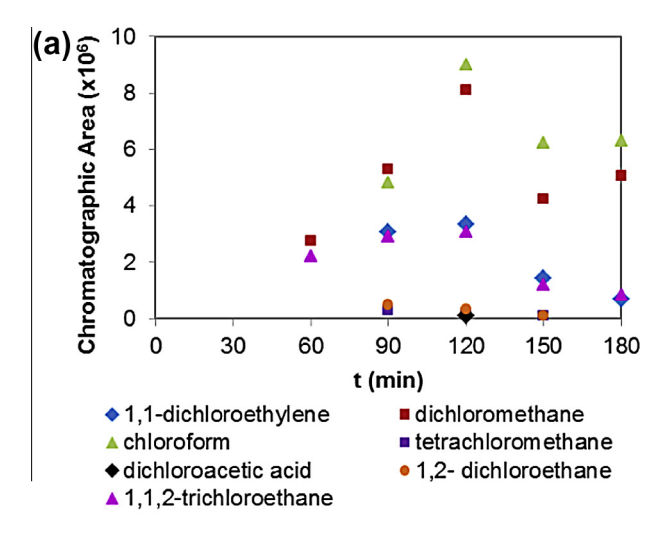


Fig. 11. Difference between measured TOC and TOC calculated from the quantified THF and intermediate compounds. The upper red line corresponds to the initial TOC value. (For interpretation of the references to color in this figure legend, the reader is referred to the web version of this article.)



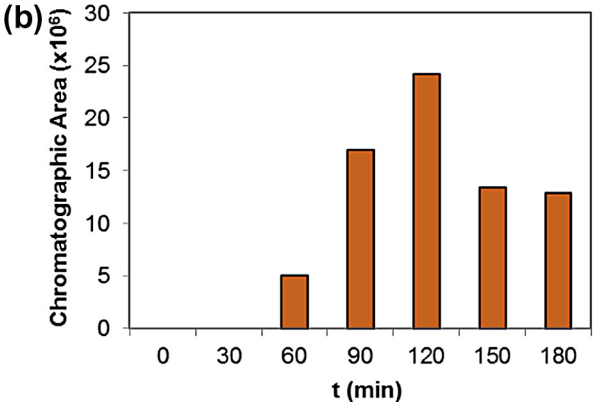


Fig. 12. Identified organochloride by-products formed during the electrolysis of THF solutions (a) and total chromatographic area provided by the total of the organochloride compounds identified (b). $j_{app} = 300 \text{ A/m}^2$. 1 g/L NaCl electrolyte solution.

together with the sum of chromatographic areas. It is observed that the global profile coincides with the shape of ΔTOC plot. In the case of chloroform, the concentration has been quantified reaching a maximum value of 3.6 mg/L, which is far less the amount required to justify ΔTOC .

4.5. Kinetic analysis

From the data discussed herein, it can be inferred that the kinetics of the oxidation process of THF on BDD anodes is strongly influenced by the applied current density and by indirect oxidation processes in the bulk solution. At this point, it is interesting to fit the COD removal data to the kinetic model formed by Eqs. (2)—

(6). The data obtained as a function of the applied current density and displayed in Fig. 4b were fitted.

The k_m value of the electrochemical cell within the fluid dynamic conditions used is 2.0×10^{-5} m s⁻¹, as calculated in the section of Theory. Taking into account the surface/volume ratio of the electrochemical cell [42], this k_m value corresponds to a kinetic constant of around 0.0168 min⁻¹. The values of the apparent kinetic constant k_1 , obtained from data fitting, and the calculated value of k, both parameters defined in Eq. (6) are given in Table 1. For $j_{app} = 300 \text{ A/m}^2$, only data obtained for experimental times after t_{cr} = 76 min were fitted to Eq. (6). For the interval between t = 0 and t_r = 76 min, data were fitted to zeroth order kinetics according to Eq. (2). The value of the apparent kinetic constant k_1 , 0.017 min⁻¹, is very close to the theoretical value derived from k_m and the anode area to treated volume ratio used in the electrolysis experiments. Increasing the applied current densities results in values of the apparent kinetic constant of 0.028 min⁻¹ (at $j_{app} = 600 \text{ A/m}^2$) and $k_1 = 0.048 \text{ min}^{-1}$ (at $j_{app} = 1200 \text{ A/m}^2$). According to Eq. (6) the difference is assigned to the enhanced secondary oxidation processes in the bulk derived from the higher concentration of electrogenerated oxidants at higher current densities, as it is characterized by increasing values of k. Fig. 4b includes the simulated results of normalized COD concentration that result from the model and parameters given in Table 1, showing the good fitting.

5. Conclusions

Several conclusions can be drawn from this work. Boron doped diamond electrodes (BDD) electrodes provided the complete removal of tetrahydrofuran (THF) contained in industrial wastewaters, and practically the total mineralization of the organic contaminant load, since TOC removals as high as 95% were easily achievable. Sodium chloride, that was compared to sodium sulfate, was selected as electrolyte due to its ready availability and its advantages in terms of the better pH development of the treated waters, although the kinetics of COD and TOC removal were equivalent for both electrolytes. It was assessed that the removal kinetics of COD and TOC were enhanced at increasing values of the applied current density. These results, together with the hydrodynamic analysis of the mass transport limitations of the electrochemical cell, revealed that the occurrence of electrogenerated oxidants in the bulk solution was likely to contribute significantly to the oxidation of THF and its intermediate products. Seven intermediate products of THF oxidation were identified; among them succinic acid was found at the highest concentrations. Chloride oxidation produced free chlorine, chlorate and perchlorate, although perchlorate formation was completely hindered at low current densities for the times needed for complete mineralization of the wastewater organic compounds. In the view of these results, it is concluded that the electrochemical oxidation on BDD anodes

 Table 1

 Kinetic parameters that characterize COD removal rate. Influence of $j_{applied}$.

j_{app} (A/m ²)	COD_0 (mgO_2/L)	$j_{lim} \over (A/m^2)$	$j_{app}/\ j_{lim}$	t _{cr} (min)	Observed kinetic regime	Apparent kinetic constant in Eq. (6) k_1 (min ⁻¹)	Calculated k parameter in Eq. (6) (min^{-1})
300	2818	676	0.44	76	Initially zeroth order First order t_{cr}	0.017	-
600	2779	667	0.88	8	Initially zeroth order First order t_{cr}	0.028	0.011
1200	2923	706	1.67	-	First order	0.048	0.031

has great potential for the practical treatment of industrial wastewaters containing high concentration of THF.

Acknowledgements

Financial support of Project ENE2010-15585 is gratefully acknowledged. P. Fernandez-Castro acknowledges a postgraduate fellowship BES-2012-054790.

References

- [1] L. Karas, W.J. Piel, Ethers, in: Kirk-Othmer Encyclopedia of Chemical Technology, John Wiley & Sons Inc., 2004.
- [2] H. Müller, Tetrahydrofuran, in: Ullmann's Encyclopedia of Industrial Chemistry, Wiley-VCH, Weinheim, 2002.
- [3] Tetrahydrofuran Global Strategic Business Report. Global Industry Analysts Inc., April 2012.
- [4] K. Verschueren, Handbook of Environmental Data on Organic Chemicals, fourth ed., vol. 2, Wiley Interscience, New York, 2001, pp. 1971–1974.
- [5] USEPA, Toxicological Review of Tetrahydrofuran (CAS No. 109-99-9), US Environmental Protection Agency, Document Reference EPA/635/R-11/006F, Washington, February 2012.
- [6] H.A. Painter, E.F. King, Ring Test Programme 1983–84; Assessment of Biodegradability of Chemicals in Water by Manometric Respirometry. EUR 9962 CA 103:182390. Contract nr XI/W/83/238. Commission of the European Communities, Water Research Centre, Elder Way, UK.
- [7] Y. Yao, J. Guan, P. Tang, H. Jiao, C. Lin, J. Wang, Z. Lu, H. Min, H. Gao, Assessment of toxicity of tetrahydrofuran on the microbial community in activated sludge, Bioresour. Technol. 101 (2010) 5213–5221.
- [8] J.M. Chen, Y.Y. Zhou, D.Z. Chen, X.J. Jin, A newly isolated strain capable of effectively degrading tetrahydrofuran and its performance in a continuous flow system, Bioresour. Technol. 101 (2010) 6461–6467.
- [9] T. Tajima, N. Hayashida, R. Matsumura, A. Omura, Y. Nakashimada, J. Kato, Isolation and characterization of tetrahydrofuran-degrading *Rhodococcus aetherivorans* strain M8, Process Biochem. 47 (2012) 1665–1669.
- [10] K.J. Daye, J.C. Groff, A.C. Kirpekar, R. Mazumder, High efficiency degradation of tetrahydrofuran (THF) using a membrane bioreactor: identification of THFdegrading cultures of *Pseudonocardia* sp. strain M1 and Rhodococcus ruber isolate M2, J. Ind. Micorbiol. Biotechnol. 30 (2003) 705–714.
- [11] D.-Z. Chem, J.-Y. Fang, Q. Shao, J.-X. Ye, D.-J. Ouyang, J.-M. Chen, Biodegradation of tetrahydrofuran by *Psudomonas oleovorans* DT4 immobilized in calcium alginate beads impregnated with activated carbon fiber: mass transfer effect and continuous treatment, Bioresour. Technol. 139 (2013) 87–93.
- [12] D.W. Green, R.H. Perry, Perry's Chemical Engineering Handbook, eighth ed., McGraw-Hill, 2007.
- [13] S. Xu, H. Wang, Separation of tetrahydrofuran-water azeotropic mixture by batch extractive distillation process, Chem. Eng. Res. Des. 84 (2006) 478-482.
- [14] A. Urtiaga, E.D. Gorri, C. Casado, I. Ortiz, Pervaporative dehydration of industrial solvents using a zeolite NaA commercial membrane, Sep. Purif. Technol. 32 (2003) 207–213.
- [15] A.B. Pereiro, J.M.M. Araújo, J.M.S.S. Esperana, I.M. Marrucho, L.P.N. Rebelo, Ionic liquids in separations of azeotropic systems – a review, J. Chem. Thermodyn. 46 (2012) 2–28.
- [16] A. M Urtiaga, E.D. Gorri, J.K. Beasley, I. Ortiz, Mass transfer analysis of the pervaporative separation of chloroform from aqueous solutions in hollow fiber devices, J. Membr. Sci. 156 (1999) 275–291.
- [17] S. Ray, S.K. Ray, Permeation studies of tetrahydrofuran-water mixtures by pervaporation experiments, Sep. Purif. Technol. 50 (2006) 156–160.
- [18] T.J. Wang, Z.H. Ma, M.Y. Huang, Y.Y. Jiang, Selective oxidation of tetrahydrofuran with molecular oxygen catalyzed by polyalumazane-platinum complexes, Polym. Adv. Technol. 7 (1996) 88–91.
- [19] M.T. Hay, S.J. Geib, D.A. Pettner, Aerobic oxidation of tetrahydrofuran by a series of iron (III) containing POSS compounds, Polyhedron 28 (2009) 2183– 2186.
- [20] B. Wermeckes, F. Beck, H. Schulz, Selective anodic oxidation of tetrahydrofuran, Tetrahedron 43 (1987) 577–583.
- [21] C. Avgousti, N. Georgolios, G. Kyriacou, G. Ritzoulis, Electrochemical oxidation of tetrahydrofuran in sulphuric acid solution, Electrochim. Acta 44 (1999) 3295–3301.
- [22] W. Schwarz, J. Schossig, R. Rossbacher, H. Höke, Butyrolactone, in: Ullmann's Encyclopedia of Industrial Chemistry, Wiley-VCH, Weinheim, 2000.
- [23] X. Li, L. Kong, Y. Xiang, Y. Ju, X. Wu, F. Feng, J. Yuan, L. Ma, C. Lu, Q. Zhang, A resource recycling technique of hydrogen production from the catalytic degradation of organics in wastewater, Sci. China, Ser. B 51 (2008) 1118–1126.
- [24] M. Mehrvar, W.A. Anderson, M. Moo-Young, Photocatalytic degradation of aqueous tetrahydrofuran, 1,4-dioxane, and their mixture with TiO₂, Int. J. Photoenergy 2 (2000) 67–80.

- [25] M. Mehrvar, W.A. Anderson, M. Moo-Young, Photocatalytic degradation of aqueous organic solvents in the presence of hydroxyl radicals scavengers, Int. J. Photoenergy 3 (2001) 187–191.
- [26] Á. Anglada, A. Urtiaga, I. Ortiz, Contributions of electrochemical oxidation to waste-water treatment: fundamentals and review of applications, J. Chem. Technol. Biotechnol. 84 (2009) 1747–1755.
- [27] M. Panizza, G. Cerisola, Direct and mediated anodic oxidation of organic pollutants, Chem. Rev. 109 (2009) 6541–6569.
- [28] C. Comninellis, G. Chen, Basic principles of the electrochemical mineralization of organic pollutants for wastewater treatment, in: Electrochemistry for the Environment, Springer, 2010.
- [29] G.V. Buxton, C.L. Greenstock, W.P. Helman, A.B. Ross, Critical review of rate constants for reactions of hydrated electrons, hydrogen atoms and hydroxyl radicals, Phys. Chem. Ref. Data 17 (1988) 513–886.
- [30] N. Bensalah, B. Louhichi, A. Abdel-Wahab, Electrochemical oxidation of succinic acid in aqueous solutions using boron doped diamond anodes, Int. J. Environ. Sci. Te. 9 (2012) 135–143.
- [31] P. Cañizares, R. Paz, C. Saez, M.A. Rodrigo, Electrochemical oxidation of alcohols and carboxylic acids with diamond anodes. A comparison with other advanced oxidation processes, Electrochim. Acta 53 (2008) 2144–2153.
- [32] A. Anglada, A. Urtiaga, I. Ortiz, Pilot scale performance of the electro-oxidation of landfill leachate at boron-doped diamond anodes, Environ. Sci. Technol. 43 (2009) 2035–2040.
- [33] A. Anglada, A.M. Urtiaga, I. Ortiz, Laboratory and pilot plant scale study on the electrochemical oxidation of landfill leachate, J. Hazard. Mater. 181 (2010) 729–735.
- [34] A. Anglada, R. Ibañez, A. Urtiaga, I. Ortiz, Electrochemical oxidation of saline industrial wastewaters using boron-doped diamond anodes, Catal. Today 151 (2010) 178–184.
- [35] V. Díaz, R. Ibáñez, P. Gómez, A.M. Urtiaga, I. Ortiz, Kinetics of electro-oxidation of ammonia-N, nitrites and COD from a recirculating aquaculture saline water system using BDD anodes, Water Res. 45 (2011) 125–134.
- [36] G. Pérez, A.R. Fernández-Alba, A.M. Urtiaga, Í. Ortiz, Electro-oxidation of reverse osmosis concentrates generated in tertiary water treatment, Water Res. 44 (2010) 2763–2772.
- [37] L. Feng, E.D. van Hullebusch, M.A. Rodrigo, G. Esposito, M.A. Oturan, Removal of residual anti-inflammatory and analgesic pharmaceuticals from aqueous systems by electrochemical advanced oxidation processes. A review, Chem. Eng. J. 228 (2013) 944–964.
- [38] A. Pérez-González, A.M. Urtiaga, R. Ibáñez, I. Ortiz, State of the art and review on the treatment technologies of water reverse osmosis concentrates, Water Res. 46 (2012) 267–283.
- [39] Standard Methods for Examination of Water and Wastewater, 20th ed., APHA, AWWA, WEF, American Public Health Association/Water Environment Federation, Washington, DC, USA, 1998.
- [40] M. Panizza, P.A. Michaud, G. Cerisola, C. Comninellis, Anodic oxidation of 2naphthol at boron-doped diamond electrodes, J. Electroanal. Chem. 507 (2001) 206–214.
- [41] M. Mascia, A. Vacca, A.M. Polcaro, S. Palmas, J.R. Ruiz, A. Da Pozzo, Electrochemical treatment of phenolic waters in presence of chloride with boron-doped diamond (BDD) anodes: experimental study and mathematical model, J. Hazard. Mater. 174 (2010) 314–322.
- [42] A. Urtiaga, I. Ortiz, A. Anglada, D. Mantzavinos, E. Diamadopoulos, Kinetic modeling of the electrochemical removal of ammonium and COD from landfill leachates, J. Appl. Electrochem. 54 (2012) 779–786.
- [43] C.R. Wilke, Pin Chang, Correlation of diffusion coefficients in dilute solutions, AlChE J. (1955) 264–270.
- [44] Manual para la gestión de vertidos. Autorización de vertido. Ministerio de Agricultura, Alimentación y Medio Ambiente (MAGRAMA), Gobierno de España, 2007. http://www.magrama.gob.es/es/agua/publicaciones/manual_para_la_gestion_de_vertidos_tcm7-28966.pdf (visited May 2013).
- [45] G. Pérez, J. Saiz, R. Ibañez, A.M. Urtiaga, I. Ortiz, Assessment of the formation of inorganic oxidation by-products during the electrocatalytic treatment of ammonium from landfill leachates, Water Res. 46 (2012) 2579–2590.
 [46] Á. Anglada, A. Urtiaga, I. Ortiz, D. Mantzavinos, E. Diamadopoulos, Boron-
- [46] A. Anglada, A. Urtiaga, I. Ortiz, D. Mantzavinos, E. Diamadopoulos, Boron-doped diamond anodic treatment of landfill leachate: evaluation of operating variables and formation of oxidation by-products, Water Res. 45 (2011) 828–838.
- [47] A. Sánchez-Carretero, C. Sáez, P. Cañizares, M.A. Rodrigo, Electrochemical production of perchlorates using conductive diamond electrolyses, Chem. Eng. J. 166 (2011) 710–714.
- [48] G. Pérez, R. Ibáñez, A.M. Urtiaga, I. Ortiz, Kinetic study of the simultaneous electrochemical removal of aqueous nitrogen compounds using BDD electrodes, Chem. Eng. J. 197 (2012) 475–482.
- [49] E.T. Urbansky, Perchlorate as an environmental contaminant, Environ. Sci. Pollut. Res. 9 (2012) 187–192.
- [50] J.M. Aquino, M.A. Rodrigo, R.C. Rocha-Filho, C. Sáez, P. Cañizares, Influence of the supporting electrolyte on the electrolyses of dyes with conductivediamond anodes, Chem. Eng. J. 184 (2012) 221–227.